FINITE ELEMENT ANALYSIS OF CONTACT AREA IN SINGLE-LAP MECHANICALLY FASTENED LAMINATED COMPOSITE PINNED JOINTS WITH DIFFERENT GEOMETRIC DIMENSIONS

F. Daneshvar [1], V. Yavari [1], M.H. Kadivar [1], I. Rajabi [2]

[1] Department of Mechanical Engineering, Shiraz University, Shiraz, Iran
Engineering School, Shiraz University, Zand Street, Shiraz 71348-51154, Iran
yavari@yavari.info

[2] Department of Mechanical Engineering, Air-naval Research Center, Shiraz, Iran
irajabi@mut-es.ac.ir

ABSTRACT

This paper presents numerical analyses for computing and evaluating the behavior of the laminated composite plate at the contact area in single lap mechanically fastened joints. A study of the effects of the stacking sequence and friction between the pin and the plate was done by Yavari et. al. [11] but steel different aspects of the problem are remained to be taken in to account. In this work different issues of mechanical engineering interests such as radial stress and radial displacement around the hole and the joint separation angle are evaluated by using commercial software ABAQUS 6.6-1[13] finite element code. Results are determined for symmetric and non-symmetric stacking sequence while the plate geometry is systematically varied. Attempts are made to validate the models with previous works. The contact is considered frictionless. Increase in plate length and thickness results in decrease of the contact.

1. INTRODUCTION

Composite materials have been used extensively in aircraft and space craft construction because of their high strength-to-weight ratio. These structural components are generally connected with other components by means of joints. Joints are necessary load transfer elements and performance of the structures is critically dependent upon the behavior of any joints they contain. Joints failure can lead to premature failure of the structure. The problem of mechanically fastened joints in composites is difficult to analyze because of the anisotropic and heterogeneous nature of the material. Mechanical fasteners such as pins, rivets and bolts are often selected due to the fact that they are easy to assemble and repair or substation. These joints require holes to be drilled in the structure, large stress concentration tends to develop around the hole which can severely reduce the overall strength of the structure.

In order to understand the behavior of composite structures to the presence of holes we need to determine the three dimensional stress distribution at the contact area and within the plate. Extensive researchers aimed at understanding of the sensitivity of composite structures weakened by an opening and deformed by forces applied to the mid plane. Experimental results are large part of literature published and effects of clearance [2] and geometry parameters [3-6] are investigated by many researchers. Analytical method was done by Madenci and Ileri [7] to predict contact stresses in mechanical joints with single fastener and a row of fasteners. Three dimensional finite element analyses was used to examine the effects of bolt-hole clearance on the behavior of composite bolted

joints by McCarthy [8]. Okutan and Karakuzu [9] investigated the effects of geometric dimensions on the strength of pinned joints and showed a definite dependence of bearing strength on stacking sequence. Dirikolu and Aktas [10, 11] determined maximum bearing strength for [90/45/-45/0] and [0/45/-45/90] pin loaded carbon composite laminates experimentally and numerically. Yavari et. al. analyzed the contact area between the pin and the hole in composite pinned joints with a three dimensional finite element model and computed the effects of stacking sequences [12] and friction [13] between the pin and the hole on the contact area.

Current paper continues the analysis of radial stresses and displacement variation and determines separation and contact angles in each ply of a composite plate at the contact area of a pinned joint. To perform this, symmetric and non-symmetric stacking sequences are used to compute separation and contact angle around the hole while geometric variations are investigated.

2. PROBLEM DEFINITION

The configuration and loading studied in the present research are shown in Fig. 1. A concentrated tensile load *P* is applied to the plate and the rigid pin which is fixed in the site, resists the load. Load is parallel to the plate and symmetric with respect to the centerline. The configuration is described by the length (*L*), the edge distance (*e*), the width (*w*), the thickness (*t*), and the hole diameter (*D*). θ is the angular coordinate. θ =0 corresponds to 9 o'clock; θ =90 corresponds to 12 o'clock and θ =±180 corresponds with 3 o'clock. Only the case of equal pin and hole radii is considered since this is sufficient for the purpose of this study. The laminates with stacking sequences of [0/45/90/-45] and [0/90/90/0] are selected for investigation. The orientation of plies in the stacking sequences is considered with respect to the positive *x*-direction. These laminates are chosen so that a variety of stress fields could be observed. For each of the laminates, three-dimensional model is used. The geometry of the plate is summarized in Table 1. The laminated composite plate is consisted of four layers with properties as in table 2. The contact is considered frictionless.

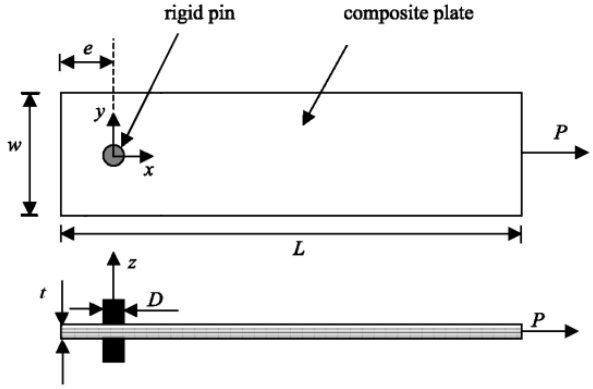

Figure 1: The geometry of the pinned joint problem.

Table 1: The geometric dimensions of the composite plate

L (mm)	e (mm)	w (mm)	t (mm)	D (mm)
280	32	32	1.61	6.8

Table 2: Elastic properties for the unidirectional lamina

E_{11} (Gpa)	E_{22} (Gpa)	E_{33} (Gpa)	G_{12} (Gpa)	G_{11} (Gpa)	G_{23} (Gpa)	ν_{12}	ν_{13}	ν_{23}
9.8	3.2	7.8	4.7	4.7	3.2	0.34	0.34	0.44

3. FINITE ELEMENT MODEL

The three-dimensional finite element model which is developed for use with the commercial software ABAQUS 6.6-1 is shown in Fig. 2. The model consists of two parts, the rigid pin and the plate. Because the effect of pin elasticity is negligible on the resulting contact stress distribution in the laminate [15], the pin circumference is modeled as a rigid surface. Instead of using solid finite element for pin, in this regard we use the ability of ABAQUS and define the pin surface as an analytical rigid surface that is more computationally efficient and will limit discretisation error. Contact pair are then defined between pin and plate surfaces. Since both the pin and the plate are stiff bodies which do not undergo large rotations with respect to the applied load a linear analysis is performed. Each ply is modeled as a row of three-dimensional linear solid elements (C3D8). The elements are finer around the hole, thereby facilitating precise computation of the contact stresses. At farther points, the reduced integration elements are applied (C3D8R). In addition to reduce the computation time, the over-estimated stiffness of the full integration elements around the hole is moderated. To define the contact of the pin and the plate, the master-slave algorithm is applied.

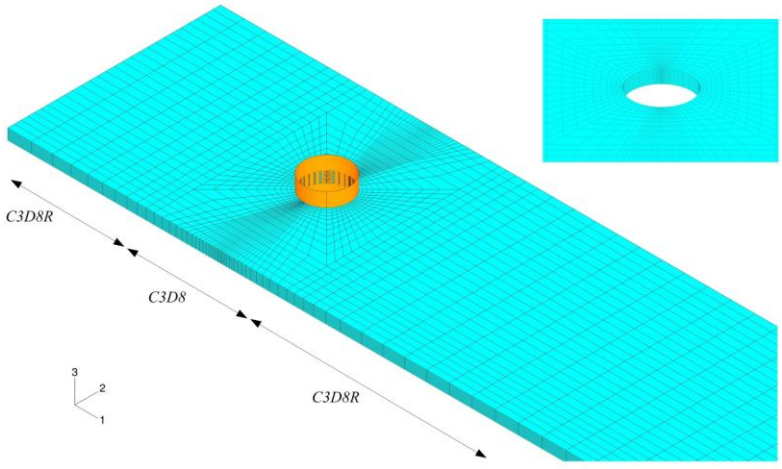

Figure 2: The three-dimensional mesh representing the problem.

In order to validate present finite element model, strains are computed along 1-direction and are compared with those obtained by Hyer [1] in Fig. 3. It is seen that the results are close to each other.

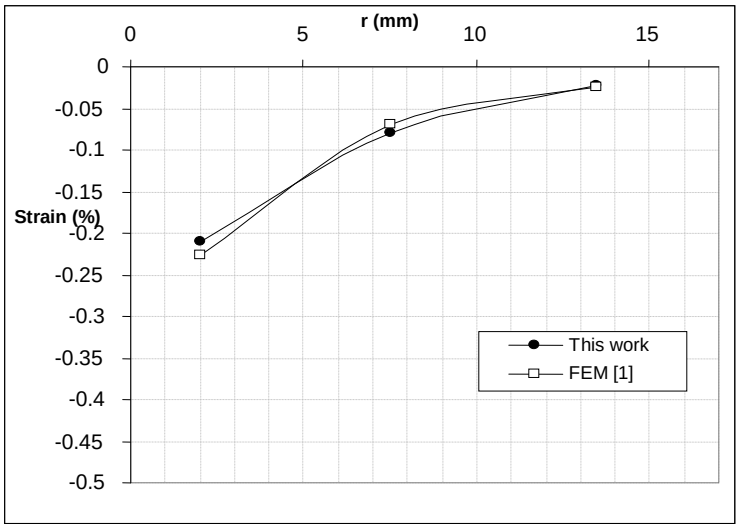

Figure 3: Comparison of present results with previous results.

4. STRESS FIELD AROUND THE HOLE

Radial stress distribution in each ply at the contact area is shown in Fig. 4. The stresses at the center of each ply are plotted. For better presentation of the figures, stresses are normalized by the average bearing stress. The average bearing stress is defined as:

$$\sigma_b = P/Dt \quad (1)$$

where P is the load , D is the hole diameter and t is the laminate thickness.

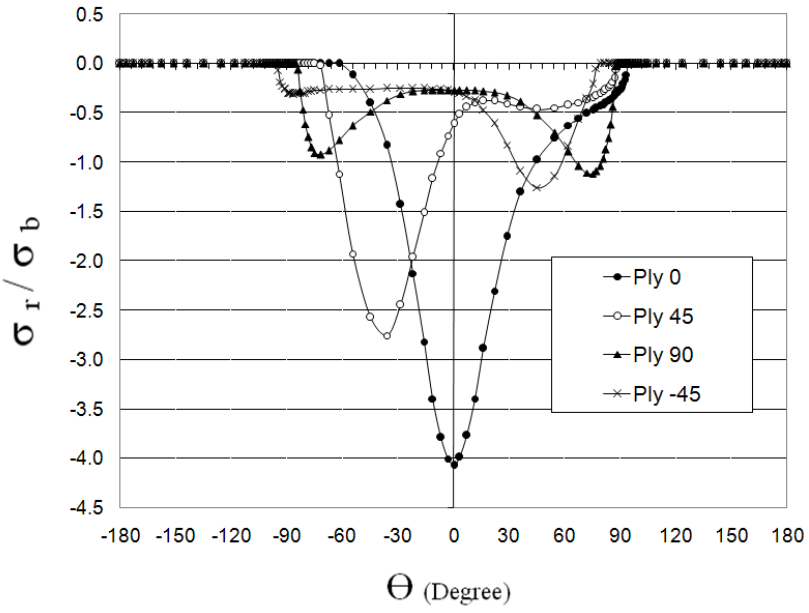

Figure 4: Normalised radial stresses around the hole for a $[0/45/90/-45]_s$ laminate

No symmetry is seen from the figure. For all of the plies the radial stress decreases around the circumference of the hole with increasing angle toward the net section where no radial load is carried by plies. The radial stresses around the hole are compressive regardless of ply orientation. From the depicted results it is obvious that the peak radial stress decreases noticeably for plies other than $\theta = 0°$. Due to high stiffness in the loading direction, the 0˚ plies are under the highest stress. High radial stress levels are also evident in the ±45˚ plies with the peak load occurring close to the respective ply fiber directions where the stiffness is high. The radial stress distribution in these plies is non-symmetric about the bearing plane ($\theta = 0°$) and the stresses in +45˚ plies are slightly higher than the -45˚ plies. The maximum radial stress in the 90˚ plies is shown to occur at $\theta_{max} = 75°$. The radial stress in 90˚ plies is significantly lower than the stresses in 0˚ and ±45˚ plies which is physically reasonable because the stiffness in the load direction is lower in 90˚ plies compared to other plies.

As mentioned before the model assumes that the pin is rigid and so that the effect of the contact is entirely conveyed in to plate deformation. Fig. 5 shows plies radial displacement distribution around the hole. The radial displacement distribution in these plies is non-symmetric about the bearing plane and the peak radial displacement varies non-linearly due to plies different orientations. As we expect maximum radial displacement occurs at plies of $\theta = 0°$ orientation and minimum radial displacement occurs at plies of $\theta = -45°$ orientation.

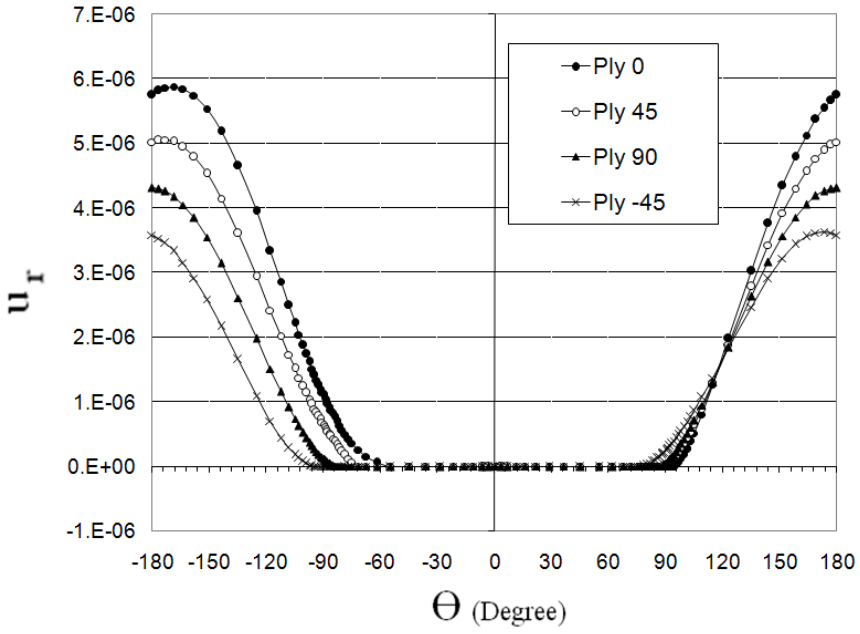

Figure 5: Radial displacements around the hole.

5. CONTACT AREA ANALYSIS

Tensile load, *P*, and existence of interaction between the pin and the plate cause the deformation in the composite plate .Separation angle is a good representative of contact

area in discussions. The total contact area is considered as summation of separation angles at both sides around the hole. As can be seen from Fig. 6, contact angle is defined as:

$\theta_c=(+\theta_s)-(-\theta_s)$

Yavari et. al [12,13] showed that separation occurs non-symmetrically around the hole. Fig. 7 shows the non-symmetric contact area for [0/45/90/-45] laminate. For laminates with different ply orientation and geometric dimensions tables 3-10 show separation (θ_s) and contact angles (θ_c). Tables 3 and 4 are effect of length on separation and contact angles for [0/45/90/-45] laminate. Results show that contact area has been enhanced up to 11˚ in -45˚ ply and 6˚ in 0˚ ply with increase in length. For 45˚ and 90˚ plies there is no noticeable change in contact area. The maximum contact area is 171˚ and occurs in 0˚ ply. The least contact area is 153˚ and occurs in -45˚ ply.

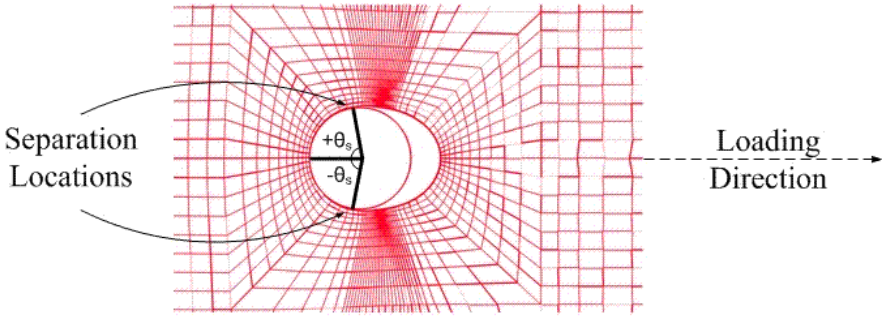

Figure 6: Separation locations around the hole.

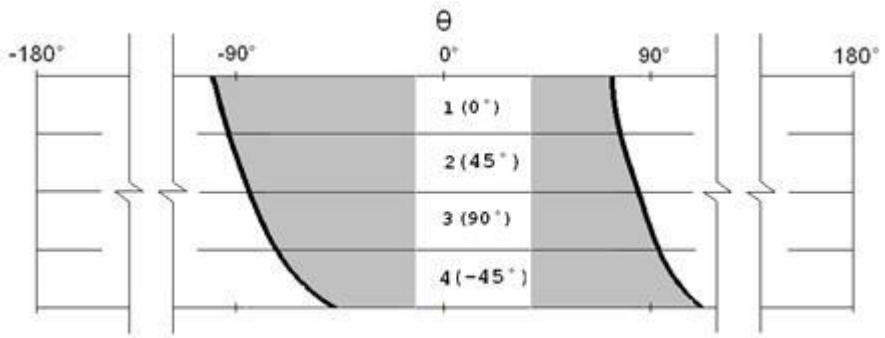

Figure 7: Contact area in [0/45/90/-45] laminate.

Table 3:
Separation and contact angles in [0/45/90/-45] laminate with L=80*mm* and t=1.6*mm*.

Ply No.	***1 (0˚)***	***2 (45˚)***	***3 (90˚)***	***4 (-45˚)***
$-\theta_s$ ***(degree)***	-91˚	-86˚	-73˚	-53˚
$+\theta_s$ ***(degree)***	74˚	80˚	85˚	100˚
$+\theta_c$ ***(degree)***	165˚	166˚	158˚	153˚

Table 4:
Separation and contact angles in [0/45/90/-45] laminate with L=280*mm* and t=1.6*mm*.

Ply No.	***1 (0˚)***	***2 (45˚)***	***3 (90˚)***	***4 (-45˚)***
$-\theta_s$ ***(degree)***	-95˚	-81˚	-69˚	-71˚
$+\theta_s$ ***(degree)***	76˚	83˚	88˚	93˚
$+\theta_c$ ***(degree)***	171˚	164˚	157˚	164˚

Table 5 shows the effect of increase in thickness on the contact area in [0/45/90/-45] laminate. As can be seen, separation and contact angles are extremely dependent to the laminate thickness. In 0˚ and 45˚ plies there is a reduction in contact area while an increase of contact area is seen in the 90˚ and -45˚ plies. Maximum contact area reduces to 167˚ and occurs in -45˚ ply. Maximum decrease in contact angles is 18˚ which occurs at 0˚ ply and an increase of 8˚ occurs at 90 ply. Tables 6-8 are effect of length and thickness on contact angles in [0/90/90/0] laminate. Because 0˚ and 90˚ plies are symmetric due to the direction of the applied load, the contact area is symmetric with respect to the load direction. Generally, increase in length and thickness decreases the contact area. The maximum contact area is 164˚ and occurs in 90˚ plies where increase in length from L=80mm to L=280mm results in 4˚ decrease in contact area. No change is seen in 0˚ plies as a results of increasing plate length.

Table 5:
Separation and contact angles in [0/45/90/-45] laminate with L=280*mm* and t=2*mm*.

Ply No.	***1 (0˚)***	***2 (45˚)***	***3 (90˚)***	***4 (-45˚)***
$-\theta_s$ ***(degree)***	-56˚	-74˚	-85˚	-95˚
$+\theta_s$ ***(degree)***	97˚	87˚	80˚	72˚
$+\theta_c$ ***(degree)***	153˚	161˚	165˚	167˚

Table 6:
Separation and contact angles in [0/90/90/0] laminate with L=80*mm* and t=1.6*mm*.

Ply No.	***1 (0˚)***	***2 (90˚)***	***3 (90˚)***	***4 (0˚)***
$-\theta_s$ ***(degree)***	-78˚	-82˚	-82˚	-78˚
$+\theta_s$ ***(degree)***	78˚	82˚	82˚	78˚
$+\theta_c$ ***(degree)***	156˚	164˚	164˚	156˚

Table 7:
Separation and contact angles in [0/90/90/0] laminate with L=280*mm* and t=1.6*mm*.

Ply No.	***1 (0˚)***	***2 (90˚)***	***3 (90˚)***	***4 (0˚)***
$-\theta_s$ ***(degree)***	-78˚	-80˚	-80˚	-78˚
$+\theta_s$ ***(degree)***	78˚	80˚	80˚	78˚
$+\theta_c$ ***(degree)***	156˚	160˚	160˚	156˚

Table 8:
Separation and contact angles in [0/90/90/0] laminate with L=280*mm* and t=2*mm*.

Ply No.	***1 (0˚)***	***2 (90˚)***	***3 (90˚)***	***4 (0˚)***
$-\theta_s$ ***(degree)***	-78˚	-80˚	-80˚	-78˚
$+\theta_s$ ***(degree)***	78˚	80˚	80˚	78˚
$+\theta_c$ ***(degree)***	156˚	160˚	160˚	156˚

Table 9 shows the respond of [0/45/90/-45] laminated composite plates to edge distance variation. Compared to the original plate of Table 4 with e=32mm we see that 0˚ and 90˚ plies are experiencing a reduction in contact area of 22˚ and 4˚ respectively. Plies of 90˚and 45˚ orientation experiencing a wider contact area with an increase in their contact area by 11˚. It is obvious from the results that 0˚ ply is most sensitive ply with 22˚ reduction in contact area.
From Table 10 which shows the respond to plate width variations except ply 0˚ other plies increase in contact area. Compared to Table 4, plies of 45˚, 90˚ and -45˚ orientation goes through an increase of contact area for 1˚, 18˚ and 16˚ respectively. 0˚ ply is contracted to 155.8 ˚ which is 17˚ less than the original plate of w=32mm.

Table 9:
Separation and contact angles in [0/45/90/-45] laminate with L=280*mm* and e=20*mm*.

Ply No.	***1 (0˚)***	***2 (90˚)***	***3 (90˚)***	***4 (0˚)***
$-\theta_s$ ***(degree)***	-56˚	-72˚	-83˚	-97˚
$+\theta_s$ ***(degree)***	93˚	88˚	85˚	78˚
$+\theta_c$ ***(degree)***	149˚	160˚	168˚	175˚

Table 10:
Separation and contact angles in [0/90/90/0] laminate with L=280*mm* and *w*=20*mm*.

Ply No.	***1 (0˚)***	***2 (90˚)***	***3 (90˚)***	***4 (0˚)***
$-\theta_s$ ***(degree)***	-59˚	-75˚	-90˚	-102˚
$+\theta_s$ ***(degree)***	97˚	90˚	85˚	78˚
$+\theta_c$ ***(degree)***	156˚	165˚	175˚	180˚

6. CONCLUSION

Radial stress, Radial displacement distributions and contact angle variations in a pinned hole are investigated numerically. From the results presented, it is clear that plate geometry and stacking sequence have a significant effect on these issues. Thereby consideration of these points can result in design of a reliable pinned connection. It is concluded that reducing length and thickness will increase the contact area.

7. NOMENCLATURE

D	Hole diameter
t	Plate thickness
w	Plate width
e	Distance to free edge
F	Applied load
L	Plate length
θ	Radial coordinate
E_{ij}, G_{ij}, ν_{ij}	Plate elastic constants
σ_b	Bearing stress
θ_s	Separation angle
θ_{max}	Maximum radial stress location
θ_c	Contact angle
σ_r	Radial stress
U_r	Radial displacement

8. REFERENCES

1. Hyer, M.W., Klang, E.C., Cooper, D.E., "The effects of pin elasticity, clearance, and friction on the stresses in a pin-loaded orthotropic plate", *Journal of Composite Materials,* 1987; 21: 190-206.
2. Kelly, G., Hallstrom, S., "Bearing strength of carbon fiber/epoxy laminates: effects of bolt hole clearance", *Composites: Part B,* 2004; 35:331-343.
3. Icten, B.M., Sayman, D., "Failure analysis of pin-loaded aluminum-glass-epoxy sandwich composite plates", *Composite Science and Technology,* 2003; 63:727-737.
4. Okutan, B., "The effects of geometric parameters on the failure strength of pin-loaded multi-directional fiber-glass reinforced epoxy laminate", C*omposites: Part B,* 2002; 33:567-578.
5. Karakuzu, R., Gulem, T., Icten, B.M., "Failure analysis of woven laminated glass-vinylester composites with pin-loaded hole", *Composite Structures, 2006; 72:27-32.*

6. Mevlut, T., Osman, A., Alaattin, A., "An experimental investigation of the bearing strength of weft-knitted 1*1 rib glass fiber composites", *Composite Structures*, 2007; 78:392-396
7. Madenci, E., and Ileri, L., "Analytical determination of contact stresses in mechanically fastened composite laminates with finite boundaries", *International Journal of Solids and Structures*, 1993; 30:2469-2484.
8. McCarthy, C.T., McCarthy, M.A., "Three-dimensional finite element analysis of single-bolt, single-lap composite bolted joints: part II- effects of bolt-hole clearance", *Composite Structures*, 2005; 71:159-175.
9. Okutan, B., karakuzu, R., "The strength of pinned joint in laminated composites", *Composites science and technology*, 2003; 63:893-905.
10. Dirikolu, M.H., Aktas, A., "The effect of stacking sequence of carbon epoxy composite laminates on pinned-joint strength", *Composite Structures*, 2003; 62:107-111.
11. Dirikolu, M.H., Aktas, A., "An experimental and numerical investigation of strength characteristics of carbon-epoxy pinned-joint plates", *Composites Science and Technology*, 2004; 64:1605-1611.
12. Yavari, V., Rajabi, I., Kadivar, M.H., "The three dimensional finite element analyses of contact area of symmetric and non-symmetric laminated composite pinned-joints", *15th Annual-International Conference on Mechanical Engineering*, Tehran, Iran, 2007; 1689:39-45.
13. Yavari, V., Rajabi, I., Kadivar, M.H., "The effect of friction on Load distribution around the hole in composite pinned connections", *ASME Pressure Vessels and Piping Division Conference*, San Antonio, Texas, 2007; 26384.
14. ABAQUS Standard User's Manual, V6.6-1.
15. Eriksson, L.I., "Contact stresses in bolted joints of composite laminates", *Composite Structures*, 1986; 6: 57-75.